

Magnetic Field Dependence of the Knight Shift in Aluminum†

H. R. KHAN, J. M. REYNOLDS, AND R. G. GOODRICH

Department of Physics and Astronomy, Louisiana State University, Baton Rouge, Louisiana 70803

(Received 3 June 1970)

The magnetic field dependence of the Knight shift in high-purity single crystals of aluminum at low temperatures shows an oscillatory behavior. The oscillations are measured for the field directed along the [111] axis of the crystal and are found to match the de Haas-van Alphen frequency of electrons on the third zone of the Fermi surface. Details of the method of analysis necessary to obtain the wave-function amplitude for this set of carriers are given.

I. INTRODUCTION

Measurements of the magnetic field dependence of the Knight shift σ have been shown to lead to detailed information about the wave functions of electrons on the Fermi surface (FS) of metals.¹ The Knight shift in high-purity single-crystal metals^{2,3} is observed to oscillate as a function of applied magnetic field at the de Haas-van Alphen (dHvA) frequency of electrons on extremal area orbits of the FS. When the amplitude of these oscillations is compared to the amplitude of the oscillations in the magnetic susceptibility, the wave-function amplitude for electrons on a particular orbit can be determined. An analysis of this type has previously been applied to cadmium¹ and the present work extends the measurements and analysis to a more free-electron-like metal, aluminum.

The possibility of σ having an oscillatory field dependence was first pointed out by Das and Sondheimer.⁴ After their initial suggestion, several investigators⁵ used free-electron models in the effective-mass approximation to calculate the magnitude of the effect. The most complete of the calculations was due to Stephen⁶ who included both the paramagnetic and diamagnetic contributions to the total amplitude. The effects of a nonzero lattice potential have been included in a calculation by Glasser⁷; however, he only gives results in the limit that the Zeeman energy of the electrons is much larger than the lattice potential, and this is not the experimental situation here. The present authors have recently suggested that the correct wave-function amplitude to be considered in the oscillatory amplitude is that of the electrons on the orbits giving rise to the oscillatory component of σ and not the average over the entire FS.¹

Metallic aluminum has been the subject of many Knight-shift investigations in recent years. In fact, it was in Al powder that Knight⁸ reported the first measurements of σ . Aluminum is a convenient metal on which to perform measurements of σ since it has an isotope which is 100% abundant (^{27}Al , $I=\frac{5}{2}$) and the metal forms in a cubic structure in which there is no quadrupole splitting of the NMR line. The portion of the FS of interest here is the third band and is well-known experimentally in addition to several theoretical models which are available in the literature. Recently,

Larson and Gordon⁹ have performed detailed dHvA studies of the third zone sheet of the FS which are in good agreement with Ashcroft's model.¹⁰ A preliminary search for oscillations in σ in Al was performed by Jones and Williams¹¹ using a point-by-point technique, and the oscillations were first reported by the current authors¹² using a field-to-frequency locked spectrometer.

In the sections which follow, the experimental technique is described, the details of the method of data analysis are presented, and the results for Al are given.

II. THEORY

It has previously been shown¹ that satisfactory agreement between the measured values of $\tilde{\sigma}$ and calculations of electronic wave-function amplitude can be obtained if one computes the ratio

$$|\tilde{\sigma}|/\sigma = (\tilde{\chi}_p/\chi_p) \langle |\psi(0)|^2 \rangle_{\text{orb}} / \langle |\psi(0)|^2 \rangle_{\text{avg}}, \quad (1)$$

where $\langle |\psi(0)|^2 \rangle_{\text{orb}}$ is the average value of the square of the wave function of electrons on the extremal area orbit giving rise to the oscillations, and $\tilde{\chi}_p$ is the amplitude of the oscillations in χ_p for the same orbit. Since $\tilde{\chi}_p/\chi_p = \tilde{\rho}/\rho$ where $\tilde{\rho}$ and ρ are the oscillatory component and the total density of states at the FS, the ratio can be computed once $\tilde{\rho}$ and ρ are known.

It should be pointed out that two effects which can contribute to $\tilde{\sigma}$ have been neglected here. Both diamagnetic and relativistic (spin-spin interactions) contributions to σ are small in Al. The theoretical calculations show that diamagnetic contributions to both σ and $\tilde{\sigma}$ are small and this has been confirmed by computer fits of our data to the expressions for $\tilde{\sigma}_p$ and $\tilde{\sigma}_d$ from Stephen's theory.⁶ Although relativistic effects give rise to a large contribution to σ in Cs,¹³ they contribute only 5% in Rb and are negligible in the lighter elements.

The amplitude of the oscillations in the density of states can be obtained from the amplitude of the dHvA effect. Falicov and Stachowiak¹⁴ have given expressions for the oscillatory part of the density of states $\tilde{\rho}$ which is obtained from their expression for the two-dimensional density of states ρ_z corresponding to a given value of the momentum in the z direction k_z . Their results, however, are for a spherical FS and the expressions are rederived here to include a more general curvature for the FS. Following the procedure given in

Ref. 14,

$$\tilde{\rho} = \frac{L_3}{2\pi} \int_{-\infty}^{\infty} \rho_z dk_z \quad (2)$$

and

$$\rho_z = \frac{L_1 L_2 m}{\pi \hbar^2} \sum_{l=-\infty}^{\infty} \exp\{il[\beta A(k_z) - \hbar^{-1} E t_1 - \pi]\}, \quad (3)$$

where $L_1 L_2 L_3$ is the volume of the sample, m the electronic mass, $\beta = \hbar c / eH$, E is the energy of an electron state, $t_1 = 2\pi l / \omega_c$, where ω_c is the electron cyclotron frequency, and a factor of 2 has been included to account for the two spin states.

Assuming that near the extremal area being measured the area varies quadratically with k_z , then

$$A(z) = A(0) + \frac{1}{2}(\partial^2 A / \partial k_z^2) k_z^2, \quad (4)$$

or letting

$$\begin{aligned} \gamma &= \frac{1}{2}(\partial^2 A / \partial k_z^2), \\ A(z) &= A(0) + \gamma k_z^2. \end{aligned} \quad (5)$$

In order to evaluate ρ_z , one must evaluate the integral

$$I = \int_{-\infty}^{\infty} \exp\{il[\beta A(0) - \hbar^{-1} E t_1 + \beta \gamma k_z^2]\} dk_z,$$

which can be integrated by means of Cornu's spiral method to yield

$$I = (\pi / l \beta \gamma)^{1/2} \exp i \{ l [\beta A(0) - \hbar^{-1} E t_1] - \frac{1}{4} \pi \}. \quad (6)$$

Using this in the expression for $\tilde{\rho}$, and after some simplification, the following is obtained:

$$\begin{aligned} \tilde{\rho} &= \frac{L_1 L_2 L_3 m}{\pi^{3/2} \hbar^2} \sum_{l=1}^{\infty} (-1)^l (l \beta \gamma)^{-1/2} \\ &\quad \times \cos\{l[\beta A(0) - \hbar^{-1} E t_1] - \frac{1}{4} \pi\}. \end{aligned} \quad (7)$$

Thus, for the $l=1$ term the magnitude of $\tilde{\rho}$ is given by

$$|\tilde{\rho}| = (L_1 L_2 L_3 m / \pi^{3/2} \hbar^2) (\beta \gamma)^{-1/2}. \quad (8)$$

The oscillatory free energy can be calculated from Eq. (5), since

$$\tilde{F} = - \int f(E, T) \tilde{\rho}(E', H) dE' dE,$$

where $f(E, T)$ is the Fermi-Dirac distribution function. It should be noted that the usual factor of 2 to account for the two spin states has been omitted here since it was included in the expression for $\tilde{\rho}$. This integral can be evaluated by standard techniques to yield

$$\begin{aligned} \tilde{F} &= \frac{L_1 L_2 L_3 m}{\pi^{3/2}} \sum_{l=1}^{\infty} (-1)^l l^{-5/2} t_1^{-2} (\beta \gamma)^{-1/2} \\ &\quad \times \frac{X_l}{\sinh X_l} \cos[l\beta A(0) - \frac{1}{4} \pi], \end{aligned} \quad (9)$$

where $X_l = \pi l \hbar^{-1} t_1 k T$. The oscillatory susceptibility as measured in the dHvA effect can now be computed

since

$$\tilde{\chi} = -H^{-1}(\partial \tilde{F} / \partial H).$$

The result is

$$\begin{aligned} \tilde{\chi} &= \frac{L_1 L_2 L_3 m}{\pi^{3/2} H^2} \sum_{l=1}^{\infty} (-1)^l l^{-5/2} t_1^{-2} \beta^{1/2} \gamma^{-1/2} \\ &\quad \times \left(\frac{X_l}{\sinh X_l} \right) \sin[l\beta A(0) - \frac{1}{4} \pi]. \end{aligned} \quad (10)$$

Taking the $l=1$ term only, one obtains finally

$$\tilde{\chi} = \frac{L_1 L_2 L_3 m}{\pi^{3/2} H^2} t_1^{-2} \beta^{1/2} \gamma^{-1/2} \frac{X_1}{\sinh X_1} \sin[\beta A(0) - \frac{1}{4} \pi]. \quad (11)$$

The free-electron value of the dHvA phase α of $\frac{1}{4}\pi$ has been used here and no effects of scattering have been included. When this phase is made variable and the Dingle factor included, the final equation for $\tilde{\chi}$ per unit volume is

$$\tilde{\chi} = \frac{m t_1^{-2} \beta^{1/2} \gamma^{-1/2}}{\pi^{3/2} H^2} \exp\left(-\frac{t_1}{2\tau}\right) \frac{X_1}{\sinh X_1} \sin[\beta A(0) - \alpha], \quad (12)$$

where τ is the usual relaxation time. We have made detailed numerical fits of Eq. (12) to our data for $\tilde{\chi}$ in order to obtain values for γ . These values were then used in Eq. (8) to obtain values of $|\tilde{\rho}|$ to be used in determining the ratio of $\tilde{\chi}_p$ to χ_p in Eq. (1).

III. EXPERIMENT

The monocrystal of aluminum used in this experiment was cut by spark erosion from a zone-refined bar ($R_{300^\circ\text{K}}/R_{4.2^\circ\text{K}} \approx 7225$) obtained from Cominco Products Inc. A parallelepiped crystal of approximate dimensions $13.5 \times 11.0 \times 6.5$ mm was cut and oriented with the $[001]$, $[110]$, and $[\bar{1}10]$ axes perpendicular to the faces. In order to increase the effective surface area exposed to the radio frequency, slots approximately 0.25 mm wide and spaced 1 mm apart were cut into the crystal. The slots were then filled with Mylar sheets and a thin coating of Q -dope applied to hold them in place. This procedure allows the sample to be handled without straining it.

Multistranded No. 34 copper wire was used to wind a rf coil on a form in which the sample could be inserted. Once the sample was inserted into the rf coil, a second rigid coil was placed around the sample to be used in the dHvA studies. The entire arrangement is shown in Fig. 1.

The sample holder used was arranged such that the sample could be oriented by x-ray backreflection techniques with the sample mounted on the holder. This allowed orientation and crystallographic axis location to within $\pm 1^\circ$. The final orientation was accomplished from the dHvA studies. The sample holder was constructed after a careful NMR study of the

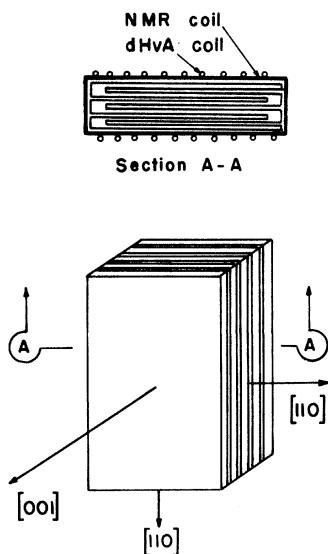


FIG. 1. Slotted NMR sample and arrangement of coils. The inside coil has its axis perpendicular to the magnetic field for the NMR measurements and the outside coil is oriented with its axis parallel to the field for the dHvA measurements. The field is applied along the $[111]$ axis.

magnetic field distribution in the Dewar to assure that the sample was located in the region of maximum field homogeneity (~ 1 part in 10^5 over the sample).

The technique for recording $\tilde{\sigma}$ has been described previously.¹² Briefly, the method consists of locking the NMR oscillator to the aluminum NMR line using a phase-sensitive detection feedback system. The magnetic field is slowly swept while σ is computed on an analog computer and recorded directly as a function of applied field. The system can detect changes in the magnitude of σ of $10^{-5}\%$. In the present experiment, the data were recorded by sweeping the field over 100 G ranges at a rate of 15 G/min. All measurements were performed at 1.1°K.

All of the dHvA measurements were performed by field modulation measurements at 1.1°K and a modulation frequency of 135 Hz. Second-harmonic detection was used and the modulation amplitude adjusted to give a maximum of $J_2(\lambda)$, the Bessel function of the first kind and of integral order 2. The argument λ here is given by $\lambda = 2\pi f/h/H^2$, where f is the dHvA frequency being measured and h the amplitude of the modulation field. The magnetic field direction could be accurately oriented to be along the $[111]$ direction in the crystal by observing the beat pattern in the dHvA output.

Since direct measurements of the dHvA amplitude were unavailable, the detection system was calibrated using cadmium samples of known dHvA amplitudes.¹ This calibration was performed by comparing the output voltage of the field modulation spectrometer between identically shaped samples of cadmium and aluminum. For the measurements on the Cd samples,

the field was directed along a direction 30° from the $[0001]$ axis in the $(10\bar{1}0)$ plane so that a single frequency due to the first band "caps" was observed. In both cases the second-harmonic voltage induced in the pickup coil is given by

$$V_2 = A J_2(\lambda) N \omega T \eta H^{-1/2} \times \frac{\exp[-k_B m^*(T+X)/H]}{1 - \exp[-2k_B m^*(T)/H]} \sin\left(\frac{2\pi f}{H} + \alpha\right),$$

where m^* is the effective-mass ratio of the orbit being observed, X the Dingle temperature, ω the modulation frequency, η the filling factor of the coil, N the number of turns on the coil, and A the amplitude of the susceptibility oscillations. Since the two orbits measured in Cd and Al have the same effective mass ($m^* = 0.150$) and the influence of the Dingle factor is small in both cases, the amplitudes could be scaled directly by proper adjustment of the modulation amplitude to maximize $J_2(\lambda)$. The calibrated amplitudes in the present case must be multiplied by a factor of 3 since there are two equivalent "cap" orbits in Cd and six equivalent γ orbits in Al which are measured. The calibrated data were recorded on an xy recorder and then punched onto cards for a least-squares fit on a digital computer to the theoretical expressions derived in Sec. II.

IV. RESULTS AND DISCUSSION

The dHvA spectrum of Al for the field ranges used in this experiment shows many frequencies giving rise to a rather complicated beat pattern. In order to analyze the oscillations in σ , it was necessary to accurately orient the field with respect to the crystallographic axis of the sample to minimize the number of observed frequencies and still have an observable

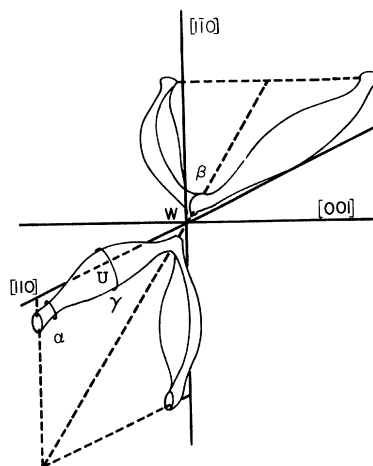


FIG. 2. Third-zone sheet of the FS of Al showing the orbits observed in this experiment.

amplitude. From the data of Larson and Gordon it is seen that with the field near 15 kG and accurately oriented along the [111] axis, there are only two observable frequencies differing in value by a factor of 10. Thus, the [111] orientation was chosen to study the σ oscillations and this direction could be accurately determined ($\pm 0.1^\circ$) by observing the beat pattern in the dHvA signals.

The oscillations observed for this field direction arise from maximum and minimum area orbits on the third band electron sheet of the FS. A sketch of this portion of the Al FS is shown in Fig. 2 along with the orbit geometry that gives rise to the oscillations. Representative recorder tracings of $\tilde{\sigma}$ in various field ranges are shown in Fig. 3 and of $\tilde{\chi}$ in Fig. 4. It should be noted that the field range over which $\tilde{\sigma}$ was recorded is small compared to the range over which $\tilde{\chi}$ is recorded. The range of observation of $\tilde{\sigma}$ is in a maximum of the beat pattern of $\tilde{\chi}$ and, for purposes of analysis, it is assumed that a single dHvA frequency is present in this field range. The observed value of this frequency is 0.348×10^7 G.

Since the absolute magnitude of $\tilde{\chi}$ was computed here, its contribution to the amplitude of $\tilde{\sigma}$ could be obtained. It was found that the oscillations in the B field in the metal contribute less than 1% of the total amplitude of $\tilde{\sigma}$.

The value of γ in Eq. (11) was obtained by performing a nonlinear least-squares fit of 51 points on the measured $\tilde{\chi}$ curves to Eq. (11). In the fitting procedure, only γ and the dHvA phase α were treated as ad-

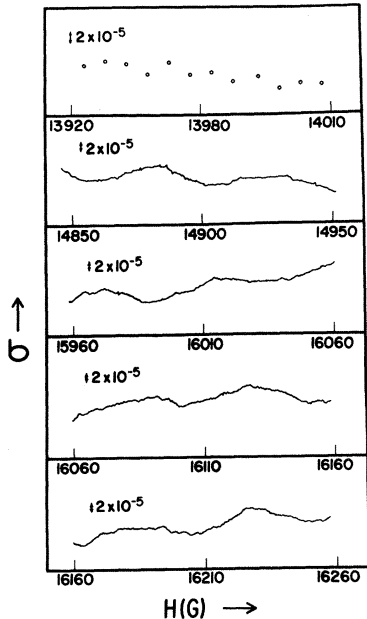


FIG. 3. Knight shift in Al versus H for several field ranges. The field is applied along the [111] axis.

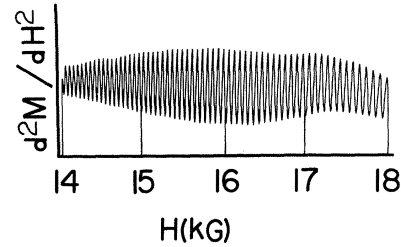


FIG. 4. de Haas-van Alphen oscillations in Al for the field along the [111] axis.

justable parameters. This led to a goodness of fit of better than 99% with the values $\gamma=26$ and $\alpha=35^\circ$. The effective mass and dHvA frequency were taken from the literature and a Dingle temperature of 0.8°K was assumed. This value of the Dingle temperature can be changed by 15% and the value of γ is changed less than 1%.

The density of states ρ was obtained from the measured values of the electronic component of the specific heat. Using the data of Howling, Mandoza, and Zimmerman,¹⁵ a value of $\rho=1.402 \times 10^{33}$ is found. The value of $\tilde{\rho}$ is computed from Eq. (8) to be $\tilde{\rho}=16.17 \times 10^{30}$. Thus,

$$|\tilde{\chi}_p|/\chi_p = |\tilde{\rho}|/\rho = 0.01153.$$

The measured value of $\tilde{\sigma}$ in the same field range as $\tilde{\rho}$ is computed is 2.15×10^{-5} while the total Knight shift is found to be $\sigma=0.162\%$ taking AlCl_3 as the reference compound. Using these numbers in Eq. (1) yields

$$\langle |\psi(0)|^2 \rangle_{\text{orb}} / \langle |\psi(0)|^2 \rangle_{\text{avg}} = 1.15 \pm 0.08$$

for the third-zone γ orbits with the field directed along the [111] axis of the crystal. The largest contribution to the error is in the measurement of $|\tilde{\sigma}|$.

A considerable error may have been made by using the value of ρ obtained from specific-heat data. The density of states obtained in this manner contains all of the renormalization effects due to electron-electron (e-e) and electron-phonon (e-p) interactions. On the other hand, how the dHvA susceptibility should be renormalized due to e-e and e-p interactions is unknown. It has tacitly been assumed here that these renormalizations cancel by taking the ratio $|\tilde{\rho}|/\rho$. If this is not the case, then up to a 40% increase in the computed value of $\langle |\psi(0)|^2 \rangle_{\text{orb}} / \langle |\psi(0)|^2 \rangle_{\text{avg}}$ would occur depending upon the degree of cancellation.

The analysis of this data is somewhat more straightforward than that previously reported for cadmium. In the present case, the average value of σ is found to be independent of applied field and the oscillations are clean in the range investigated. There is the problem, however, of a second low-amplitude frequency being mixed with the observed frequency. The data as given here will be compared to point-by-point calculations

of the wave-function amplitude over the FS when they become available. Since all of the calculations of the amplitude of $\tilde{\sigma}$ involve approximations which either eliminate the details of the wave-function amplitude completely or are not applicable to this case, there has been no attempt to make detailed comparisons to them. It is hoped that these measurements and others will stimulate more detailed theoretical studies of the effect.

ACKNOWLEDGMENTS

The authors are indebted to Dr. S. A. Khan for his help in all phases of this work. One of the authors (H.R.K.) wishes to acknowledge assistance from the Dr. Charles E. Coates Memorial Fund of the L.S.U. Foundation, donated by George H. Coates, for assistance in the publication of this manuscript.

[†] Work performed under the auspices of the U.S. Atomic Energy Commission; A. E. C. Report No. ORO-3087-39 (unpublished).

¹ R. G. Goodrich, S. A. Khan, and J. M. Reynolds, Phys. Rev. Letters **23**, 767 (1969).

² J. M. Reynolds, R. G. Goodrich, and S. A. Khan, Phys. Rev. Letters **16**, 609 (1966).

³ S. A. Khan, J. M. Reynolds, and R. G. Goodrich, Phys. Rev. **163**, 579 (1967).

⁴ T. P. Das and E. H. Sondheimer, Phil. Mag. **5**, 529 (1960).

⁵ J. I. Kaplan, J. Phys. Chem. Solids **23**, 826 (1962); S. Rodriguez, Phys. Letters **4**, 306 (1963); D. G. Dolgoplov and P. S. Bystrik, Zh. Eksperim. i Teor. Fiz. **46**, 593 (1963) [Soviet Phys. JETP **19**, 404 (1964)].

⁶ M. J. Stephen, Phys. Rev. **123**, 126 (1961).

⁷ M. L. Glasser, Phys. Rev. **150**, 234 (1966).

⁸ W. D. Knight, Phys. Rev. **76**, 1259 (1949).

⁹ C. O. Larson and W. L. Gordon, Phys. Rev. **156**, 703 (1967).

¹⁰ N. W. Ashcroft, Phil. Mag. **8**, 2055 (1963).

¹¹ E. P. Jones and D. L. Williams, Can. J. Phys. **42**, 1499 (1964).

¹² R. G. Goodrich, H. R. Khan, S. A. Khan, and J. M. Reynolds, Rev. Sci. Instr. **41**, 245 (1970).

¹³ L. Tterlikkis, S. D. Mahanti, and T. P. Das, Phys. Rev. **178**, 630 (1969).

¹⁴ L. M. Falicov and H. Stachowiak, Phys. Rev. **147**, 505 (1966).

¹⁵ D. H. Howling, E. Mandoza, and J. E. Zimmerman, Proc. Roy. Soc. (London) **A229**, 86 (1955).

Inelastic Electron Scattering and the Lorenz Ratio of Liquid Metals

M. J. RICE

General Electric Research and Development Center, P.O. Box 8, Schenectady, New York 12301

(Received 5 August 1970)

Recent experimental work has led to the surprising conclusion that the Lorenz ratios of some of the liquid metals exhibit substantial negative deviations from the ideal Sommerfeld value, hence indicating that inelastic electron scattering effects may be an important factor in some liquid metals. Motivated by these observations, we present in this paper a calculation of the electronic transport properties of a liquid metal, which takes into account the effects of inelastic electron scattering from the ionic density fluctuations to leading order in the small dimensionless parameter $E_0/k_B T$. Here E_0 denotes a typical inelastic energy transfer and $k_B T$ the Boltzmann factor. This calculation, based on the nearly-free-electron model, is carried through by use of the exact sum rules of Placzek and of de Gennes on the dynamic structure factor $S(q, \omega)$ of the classical ionic liquid component of the metal. The effects of inelastic electron scattering on the electrical resistivity are found to be negligible. Non-negligible corrections, however, associated with small-angle inelastic processes, are found to enter the electronic thermal resistivity. The corresponding depression in the Lorenz number is expressed in terms of the electron-ion pseudopotential, the static liquid structure factor, and the collective-mode frequencies associated with the density fluctuations of the liquid component. Inspection of the theoretical expression for the deviation in the Lorenz ratio reveals, however, that it is too small to account for the experimentally observed deviations. It is concluded that, within the framework of the nearly-free-electron theory, the effects of inelastic electron scattering are not the dominant cause of the rather large anomalies in the observed Lorenz ratios.

I. SYNOPSIS

In the currently existing nearly-free-electron theory¹⁻⁴ of the electronic transport properties of liquid metals, the electrons are considered to be scattered *elastically* from the ionic density fluctuations of the liquid component of the metal. A simple, but important, consequence of this approximation is that the electronic thermal conductivity κ_e is related to the electrical resistivity ρ by means of the Wiedemann-Franz relation⁵

$$\rho \kappa_e / T = L_0 = \frac{1}{3} \pi^2 (k_B / e)^2.$$

Recent experimental data for several liquid metals show, however, significant negative deviations of the Lorenz ratio $L = \rho \kappa_e / T$ from the ideal Sommerfeld value L_0 . For example, Yurchak and Smirnov⁶ and Duggin⁷ have observed a deviation in the Lorenz ratio of liquid Ga of the order of -20% , while Filippov⁸ has reported deviations in liquid Sn and Pb of the order of -30 and -12% , respectively. Deviations varying between -20 and -40% were reported for Cu some time ago.⁹ Moreover, these deviations may be a fairly strong function of temperature.^{8,9,10} Such *negative*